Drug Design, Development and Therapy

Dovepress
open access to scientific and medical research

Open Access Full Text Article

ORIGINAL RESEARCH

Huang Gan Formula Alleviates Systemic Inflammation and Uremia in Adenine-Induced Chronic Kidney Disease Rats May Associate with Modification of Gut Microbiota and Colonic Microenvironment

Jingqian Zhao[1,2,*], Chenyu Zhao[1,3,*], Tianrong Xun[1], Xiaokang Wang[1], Sui Wei[1,3], Chunxiao Ye[1], Mimi Zhang[1], Dan Guo[4], Xixiao Yang[1]

[1]Department of Pharmacy, Shenzhen Hospital, Southern Medical University, Shenzhen, People's Republic of China; [2]School of Traditional Chinese Medicine, Southern Medical University, Guangzhou, People's Republic of China; [3]School of Pharmaceutical Sciences, Southern Medical University, Guangzhou, People's Republic of China; [4]Department of Pharmacy, Nanfang Hospital, Southern Medical University, Guangzhou, People's Republic of China

*These authors contributed equally to this work

Correspondence: Dan Guo; Xixiao Yang, Email nfyyyxb@smu.edu.cn; yaxx@smu.edu.cn

Purpose: This study aims to investigate the effects of Huang Gan formula (HGF), a Chinese herbal prescription used for chronic kidney disease (CKD), on the regulation of the gut microbiota and colonic microenvironment of CKD.

Methods: CKD rats were induced by 150 mg/kg adenine gavage for 4 weeks, then orally treated with or without 3.6 g/kg or 7.2 g/kg of HGF for 8 weeks. The renal function and structure were analyzed by biochemical detection, hematoxylin and eosin, Masson's trichrome, Sirius red and immunochemical staining. Average fecal weight and number in the colon were recorded to assess colonic motility. Further, the changes in the gut microbiota and colonic microenvironment were evaluated by 16S rRNA sequencing, RT-PCR or immunofluorescence. The levels of inflammatory cytokines, uremic toxins, and NF-κB signaling pathway were detected by RT-PCR, ELISA, chloramine-T method or Western blotting. Redundancy analysis biplot and Spearman's rank correlation coefficient were used for correlation analysis.

Results: HGF significantly improved renal function and pathological injuries of CKD. HGF could improve gut microbial dysbiosis, protect colonic barrier and promote motility of colonic lumens. Further, HGF inhibited systemic inflammation through a reduction of TNF-α, IL-6, IL-1β, TGF-β1, and a suppression of NF-κB signaling pathway. The serum levels of the selected uremic toxins were also reduced by HGF treatment. Spearman correlation analysis suggested that high-dose HGF inhibited the overgrowth of bacteria that were positively correlated with inflammatory factors (eg, TNF-α) and uremic toxins (eg, indoxyl sulfate), whereas it promoted the proliferation of bacteria belonging to beneficial microbial groups and was positively correlated with the level of IL-10.

Conclusion: Our results suggest that HGF can improve adenine-induced CKD via suppressing systemic inflammation and uremia, which may associate with the regulations of the gut microbiota and colonic microenvironment.

Keywords: chronic kidney disease, systemic inflammation, colonic microenvironment, gut-kidney axis

Introduction

Chronic kidney disease (CKD) is characterized by progressive and irreversible loss of nephrons and functional impairment and is believed to become the fifth-leading global cause of death by 2040.[1] CKD may increase the risks of various comorbidities, such as cardiovascular disease, bone and mineral disorder, and anemia.[1] Although renin–angiotensin system inhibitors are used to treat kidney diseases, cardiovascular events remain a major cause of death in CKD.[2] Current studies indicate that a deteriorated blood environment may be an important factor that induces CKD-related complications. Therefore, interventions that help to purify the blood are necessary.

Received: 30 May 2023
Accepted: 24 December 2023
Published: 6 January 2024

Systemic inflammation and uremia are key features of deteriorated blood environment in CKD. They not only hinder the treatment of CKD itself through altering therapy drug metabolism,[3] but also trigger other diseases. It is believed that the inflammation originates from the cascade amplification of inflammatory response in the damaged kidney.[4] However, recent studies have found that systemic inflammation and uremia in CKD is associated with microbial dysbiosis and an impaired intestinal barrier.[5–7] During CKD, there are characteristic changes in the composition of gut flora, with bacteria in the colon producing more uremic toxins (or their precursors) during proteolysis.[8] These metabolites, which were originally removed by the kidney, accumulate in circulation because of reduced renal function. Studies have shown that these compounds are cytotoxic and can destroy normal colonic barrier. For example, indoxyl sulfate (IS) can suppress the expression of tight junction-related genes and increase the permeability of the intestinal barrier.[9] Further, impairment of the barrier leads to easy entry of bacterial components (eg, endotoxins) into the intestinal lamina propria and blood. When exposed to endotoxins, innate immune cells are stimulated and induce an inflammatory response through Toll-like receptor 4, leading to the activation of NF-κB and an inflammatory cytokine storm.[10] Together, these events contribute to the chronic inflammation and uremia in CKD's progression. Therefore, regulating intestinal microenvironment to reduce toxin synthesis and/or increase toxin excretion may be a novel strategy for CKD treatment.

Natural products from herbs have been reported to show beneficial effects on CKD via regulating the microbiota.[11,12] Huang Gan formula (HGF) is a herbal prescription developed to treat chronic renal failure and has been used in our hospital for several years. In our previous studies, we focused on the direct reno-protective effects of HGF and found that they can be achieved by suppressing renal oxidative stress and fibrosis.[13,14] However, the above evidence has highlighted a reciprocal causation between the deteriorated intestinal status and the progression of CKD. Notably, oxidative stress and fibrotic signaling pathways can be induced by toxins that are highly produced in the lumen of CKD.[15] In our clinical practice, oral administration is still the main route of administration, which provides a cozy space-time for the herbs to "intimate" with gut microbiota. Therefore, this study aims to reveal the effects of HGF on the colonic and blood environments in the context of CKD. Based on an adenine-induced CKD rat model, we investigated the protective effect of HGF on the damaged rat kidney. After HGF treatment, systemic inflammation, uremia, changes in gut microbiota and colonic environment in CKD rats were also evaluated. Further, correlation analysis was used to assess whether HGF's renoprotection correlates to gut microbiota modulation.

Materials and Methods

Reagents

Adenine (A6279, purity > 99%), aloe-emodin (A800925, 95.0%), emodin (E808871, 98.0%), rhein (R817294, 98.0%) and chrysophanol (D806395, 97.0%) were purchased from Macklin (Pudong, Shanghai, China). Kits of hematoxylin and eosin (H&E) (G1005), Masson (G1006), and Sirius red staining (GC307014) were provided by Servicebio Technology Co., Ltd (Wuhan, Hubei, China). Commercial kits of serum creatine (SCR) (C011), uric acid (UA) (C012), blood urea nitrogen (BUN) (C013) and total cholesterol (T-CHO) (A111) were purchased from Nanjing Jiancheng Bioengineering Institute (Nanjing, Jiangsu, China). Reagents for total RNA extraction (R0026), cDNA synthesis (D7185) and SYBR Green dye (D7265) were purchased from Beyotime Biotechnology (Songjiang, Shanghai, China). ELISA kits for TNF-α (0180R2), IL-6 (0190R2), IL-1β (0047R2), IL-10 (0195R2), indoxyl sulfate (IS) (70475R2), p-cresol sulfate (PCS) (70627R2) and endotoxin (0367R2) were provided by Meimian Industrial Co. Ltd. (Yancheng, Jiangxi, China). Primary antibodies, including fibronectin (GB11022), type I collagen (GB13091), ZO-1 (GB111981), and occludin (GB111401), were purchased from ServiceBio Technology Co., Ltd (Wuhan, Hubei, China). TNF-α (60291), IL-6 (21865), TGF-β1 (21898) and GAPDH (60004) were purchased from ProteinTech Groups (Wuhan, Hubei, China). NF-κB (8242S), p-NF-κB (3033S), IκBα (4814) and p-IκBα (2869) were purchased from Cell Signaling Technology (Beverly, Massachusetts, USA).

Preparation of Huang Gan Formula

Dry HGF powder was produced by Jiangxi Bencao Tiangong Technology Co., Ltd (Nanchang, Jiangxi, China). The herbs in HGF and production process of the powder were strictly in accordance with the requirements of the Chinese Pharmacopoeia (Version 2020). The batch number of the HGF powder in this study is 202120712. In brief, the extract

was prepared in boiling water three times for one-hour each time. After filtration, the filtrate was concentrated to a density of 1.10~1.15 under reduced pressure. An appropriate number of pharmaceutical excipients were dissolved in water and mixed with the filtrate. After sieving, the mixture was powdered and stored at room temperature. Before treatment, the powder was completely dissolved in warm drinking water using a magnetic agitator. HGF solution was freshly prepared daily.

Animal and HGF Treatment

Specific pathogen-free Sprague-Dawley male rats (220–250 g) were provided by Southern Medical University (Guangzhou, Guangdong, China). The rats were housed at room temperature (25 ± 5°C), stable humidity (55 ± 10%), and under a 12:12h light–dark cycle (7:00am-7:00pm) at the Animal Experimental Center of Shenzhen Hospital of Southern Medical University (Baoan, Shenzhen, China). The animal experimental procedures strictly complied with all relevant ethical rules of the Shenzhen Hospital (Approval NO. 2021–0077).

Following adaptive feeding for 1 week, the rats were randomly divided into four groups: 1) CON group (distilled water); 2) CKD group (150 mg/kg/d adenine); 3) CKD+HGF-L group (3.6 g/kg/d HGF) and 4) CKD+HGF-H group (7.2 g/kg/d). Oral administration of adenine was for 4 weeks, and HGF solution was administered for 8 weeks. The flowchart of the animal experiments is shown in Figure 1A.

In the fourth week, whole blood was collected by retro-orbital puncture after anaesthetization using isoflurane. In the end, the rats were euthanized with pentobarbital sodium (150 mg/kg) intraperitoneally after fasting overnight. Blood samples were collected from abdominal artery. After coagulation overnight at 4°C, the blood was centrifuged at 4°C and 3000 g for 10 min to collect serum. The serum was further divided into three parts and stored at −80°C for biochemistry and cytokine analysis. Then, both the left and right kidneys were weighed, and one-half of one kidney was placed in 4% paraformaldehyde for histological analyses. One-cm colon samples were fixed in the stationary fluid for histological and immunofluorescence analyses. The rest of the renal and colon tissues were immediately frozen using liquid nitrogen and stored at −80°C for further biochemical analyses.

Serum Biochemistry Assays

The serum levels of SCR, BUN, UA, and T-CHO were detected using enzymatic methods based on protocols from the manufacturer.

Serum Cytokine and Uremic Toxin Detection

The levels of endotoxin, TNF-α, IL-6, IL-1β, IL-10, IS, and PCS were determined by using the commercial ELISA kits. Briefly, aliquots of 50 μL standard solution and 50 μL serum samples were added to 96-well plates coated with rat primary antibodies. After the addition of 100 μL of HRP-conjugated reagent to each well, the well was incubated at 37°C for 60 min. We then washed and dried the wells five times, added 50 μL of chromogen solutions A and B, and incubated them at 37°C for 15 min. After 50 μL stop solution was added to stop the reaction, optical density (OD) values (450nm) were measured using a microplate reader. The concentrations of the cytokines were calculated using a standard curve.

The concentration of advanced oxidative protein products (AOPPs) in serum was detected as described in our published article.[16] Briefly, 200 μL aliquots of chloramine-T (0, 20, 40, 80, and 100 μM), 200 μL of serum samples, and 200 μL PBS were added to a 96-well plate. Potassium iodide (10 μL, 1.16 mol/L) and acetic acid (20 μL) were then added to each well. The OD values at 340 nm were measured immediately. The concentration of AOPPs was expressed as micromoles per liter of chloramine-T equivalent.

Histopathology Analysis

The renal tissues were placed in paraffin, cut into slices (4μm) and processed with HE, Masson's trichrome, or Sirius Red staining reagents. For Masson's trichrome and Sirius Red staining, fibrotic areas of the kidneys were quantified using the ImageJ software.[17] Blue and red indicate positive areas for Masson and Sirius Red staining, respectively. The areas of the blue, red, and total sections were measured, and the percentage of blue or red to total areas was calculated.

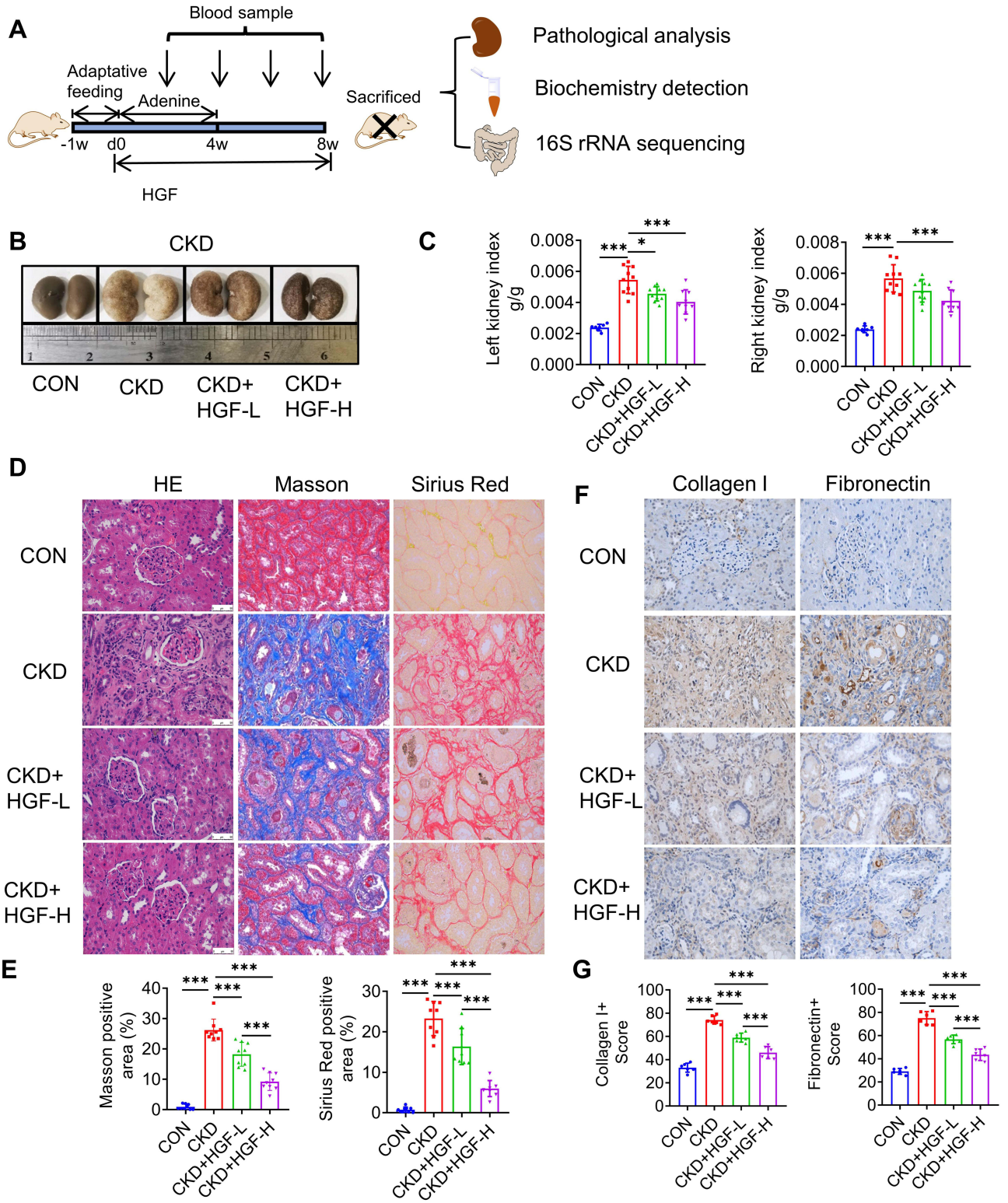

Figure 1 HGF ameliorates renal structure and function of rats with CKD. (**A**) Schematic diagram of the experiments. (**B**) Representative pictures of the kidneys. (**C**) The left and right kidney indexes. n = 7–10 rats per group. (**D** and **E**) Representative photomicrographs of H&E, Masson, and Sirius Red stains (400×) (**D**), and areas of collagen fiber quantified by ImageJ software (**E**). n = 7–9 rats per group. (**F** and **G**) Immunochemistry of fibronectin and type I collagen in the renal tissues (400×) (**F**), and positive expressions were quantified by ImageJ software (**G**). n= 7–9 rats per group. Data are presented as mean ± SD. *$P < 0.05$ and ***$P < 0.001$.

Immunohistochemistry and Immunofluorescence

For immunohistochemical analysis, the renal slices were deparaffinized, rehydrated, and rinsed. Slices were washed with citric acid buffer and heated to achieve antigen retrieval. Endogenous peroxidase activity was blocked using 3% hydrogen peroxide and incubated at room temperature. After washing with phosphate-buffered saline, slices were covered with 3% bovine serum albumin (BSA) at room temperature. The sections were then incubated with the following primary and secondary antibodies: fibronectin (1:500) and type I collagen (1:200) at 4°C overnight. Diaminobenzidine was used to visualize the reaction. Nuclei were counterstained with hematoxylin. Dehydrate the slices and secure them with neutral glue.

For immunofluorescence, after deparaffinization, antigen retrieval and sealing, ZO-1 (1:3000) and occludin (1:200) were used as primary antibodies to incubate colonic tissue slices. The slices were then immersed in secondary antibodies. Images were obtained, and the positive areas were quantified using ImageJ (Fiji) software as previously described.[18]

Western Blotting Analysis

Renal tissues were crushed in a RIPA lysis buffer, which contains 1.0 mM protease and phosphatase inhibitor cocktail. The lysate was centrifuged, and the total protein content was determined using the BCA method. Fifty micrograms of denatured protein was separated by SDS-PAGE and transferred to PVDF membranes. The membranes were blocked with 5% non-fat milk (for proteins) or BSA (for phosphorylated proteins) in 0.1% TBST for 1.5 h at room temperature. The membranes were then incubated overnight at 4°C with the following primary antibodies: TNF-α (1:1000), IL-6 (1:1000), TGF-β1 (1:1000), GAPDH (1:5000), NF-κB (1:1000), p-NF-κB (1:1000), IκBα (1:1000), and p-IκBα (1:1000). HRP-conjugated goat anti-rabbit/mouse antibody (1:5000) was used to incubate the membranes at room temperature for 1.5 h. Lastly, the protein bands were visualized using enhanced chemiluminescence, and the integral density of the target protein bands was calculated using ImageJ software.

RNA Extraction and Quantitative Real-Time PCR (RT-PCR)

The total RNA from renal tissues was extracted using an RNA extraction kit. Thereafter, the total RNA concentration was determined, and the RNA was used to synthesize cDNA. Finally, RT-PCR was performed with a 20 μL mixture. The recommended procedures were then applied. Relative mRNA expression was calculated using the CT method and normalized to GAPDH expression. Primers used in this study are listed in Table 1.

16S rRNA Sequencing Analysis

In the fourth and eighth weeks, fecal samples were collected and stored at −80°C. Bacterial DNA was extracted, and the forward primer 338F (5′-ACTCCTACGGGAGGCAGCAG-3′) and reverse primer 806R (5′-GGACTACHVGGGTWTCTAAT-3′) were used to amplify the V3-V4 region of the microbial genes. Sequencing data were processed using the Illumina MiSeq sequencing platform of Major Bio-Pharm Technology (Pudong, Shanghai, China). The alpha and beta diversities were generated using this platform. The "ggplot2" package of R software (https://www.r-project.org/) was used to generate principal coordinate analysis (PCoA) plots. Multistage taxa difference discriminant analysis was performed using Linear discriminant analysis Effect Size (LEfSe) (http://huttenhower.sph.harvard.edu/galaxy/). Only the average relative abundances were greater than 0.01%, and the bacterial taxa that reached the linear discriminant analysis (LDA) threshold (4.0) are shown. Comparisons between the two groups were further analyzed using Statistical Analysis of Metagenomic Profiles (STAMP) software. RDA plots, correlations

Table 1 Primer Sequences for RT-PCR

Gene	Forward	Reverse
TGF-β1	5′-GCCAGATCCTGTCCAAACTAA-3′	5′-TTGTTGCGGTCCACCATTA-3′
TNF-α	5′-GTCTGTGCCTCAGCCTCTTC-3′	5′-TGGAACTGATGAGAGGGAGC-3′
IL-6	5′-CACTTCACAAGTCGGAGGCT-3′	5′-TCTGACAGTGCATCATCGCT-3′
ZO-1	5′-TCGAGGTCTTCGTAGCTCCA-3′	5′-GCAACATCAGCAATCGGTCC-3′
Occludin	5′-TTCTGTGCTCACAGGTGGTT-3′	5′-TGGGCTGGATGCCAATTTAGT-3′
GAPDH	5’-ACTCTCTTCTTCCCCCTTGC-3’	5’-TCCACGACATACTCAGCAC-3’

between differentially abundant bacterial genera (top 20), and concentrations of inflammatory cytokines or uremic toxins were determined using the free Majorbio Cloud Platform (https://cloud.majorbio.com/). Accession number PRJNA847394 identifies all raw sequences in the NCBI Sequence Read Archive.

Statistical Analysis

The experimental data were analyzed using GraphPad Prism software (version 8.0). An unpaired two-tailed Student's *t*-test was used to compare two independent groups. For comparisons between more than two groups, one-way ANOVA was performed, followed by Sidak or Dunnett's test. Data are presented as the mean ± standard deviation (SD). $P < 0.05$ was considered statistically significant.

Results

Quality Control of HGF

In our previous study, we have systematically described chem-profiles of HGF and identified the chemical composition of its extract using HPLC-Q-TOF-MS.[14] Eight major compounds were identified, namely iquiritin, tectoridin, luteolin, aloe-emodin, rhein, emodin, chrysophanol, and physcion. Further, total anthraquinones (TA) in HGF (aloe-emodin, rhein, emodin and chrysophanol) were preferred as the quality control method in this study (Figure S1). All four anthraquinones are shown in the HPLC-chromatogram of HGF solution, which was same as in previous studies. The retention time of aloe-emodin, rhein, emodin and chrysophanol are approximate 20, 30, 54 and 65 min, respectively (Figure S1). Based on the standards, the quantity of the total anthraquinones of HGF in this study was 3.96 mg/g.

HGF Administration Ameliorated Renal Injury Induced by Adenine

To determine the role of HGF in renal function, we treated male SD rats with adenine for 4 weeks and with or without HGF treatment for 8 weeks (Figure 1A). We observed significant weight loss, polydipsia, and polyuria in CKD rats (Table 2); however, HGF did not alter these trends. SCR, BUN, UA, and T-CHO levels were significantly increased in CKD rats, indicating impaired renal function (Table 2). These changes were reversed by HGF treatment, with a more powerful efficacy observed in the HGF-H group (Table 2).

As for renal structure, significant renal hypertrophy was observed in the CKD group, which was improved by HGF treatment, with high-dose HGF treatment being more potent than low-dose treatment (Figure 1B and C). Compared with the CON group, CKD resulted in extracellular matrix expansion in the renal tissues. Masson and Sirius Red staining suggested that the percentage of collagen fibers was significantly higher in the renal interstitium (Figure 1D and E). In contrast, HGF treatment inhibited both matrix deposition and fibrosis. In addition, immunohistochemistry revealed a larger fibrotic area in the renal tissue of CKD rats, as evidenced by the high expression of fibronectin and type I collagen (Figure 1F). However, HGF treatment reversed this effect in a dose-dependent manner (Figure 1F and G). These results suggest that HGF can improve renal function and structure of adenine-induced CKD.

To test whether TA behaves similarly to reno-protective effects with the HGF-H group, CKD rats were treated with a mix of aloe-emodin, emodin, rhein and chrysophanol. As shown in Figure S2, TA treatment tended to reduce the renal

Table 2 General Status and Biochemical Indices

Parameters	CON	CKD	CKD + HGF-L	CKD + HGF-H
Number	7	10	7	9
Body weight (g)	401.7 ± 26.42	357.2 ± 26.86 *	377 ± 34.88	378 ± 35.03
Water intake (mL)	38.8 ± 1.626	60.17 ± 3.496***	76.42 ± 2.2***	64.33 ± 1.817***
SCR (μmol/L)	36.98 ± 5.589	96.77 ± 10.16***	76.24 ± 19.33$^{\#}$	53.69 ± 17.81$^{\#\#\#\Delta}$
BUN (μmol/L)	5.507 ± 0.9044	16.51 ± 2.655***	15.78 ± 4.369	8.087 ± 1.704$^{\#\#\#\Delta\Delta\Delta}$
UA (μmol/L)	28.57 ± 7.472	53.97 ± 11.88***	32.41 ± 14.24$^{\#\#}$	35.19 ± 8.364$^{\#}$
T-CHO (mmol/L)	1.215 ± 0.1931	2.335 ± 0.3012***	1.912 ± 0.3783$^{\#}$	1.838 ± 0.253$^{\#\#}$

Note: *$P < 0.05$ and ***$P < 0.001$ compared with CON group. $^{\#}P < 0.05$, $^{\#\#}P < 0.01$, and $^{\#\#\#}P < 0.001$ compared with CKD group. $^{\Delta}P < 0.05$ and $^{\Delta\Delta\Delta}P < 0.001$ compared with CKD + HGF-L group.

index of the CKD rats, but there is no significant difference when compared with CKD group (Figure S2A and S2B). However, the levels of SCR and BUN were significantly decreased by TA treatment (Figure S2C and S2D). TA could also reduce the infiltration of inflammatory cells and the deposition of collagen in renal interstitials (Figure S2E and S2F). These results show that TA also has reno-protective effects, and the renoprotection of HGF at least partially depends on TA.

Treatment with HGF Improved the Gut Microbial Dysbiosis Induced by CKD

As the results suggested that HGF-H had a more powerful reno-protective effect, we performed stool 16S rRNA sequencing to identify the gut microbial differences among the CON, CKD and HGF-H groups in the fourth and eighth weeks. The Shannon index, used to indicate the alpha diversity of the gut flora, was significantly higher in the CKD group at the fourth weeks. However, HGF-H treatment decreased this index in the fourth week but not eighth week (Figure 2A and 2E). We also performed principal coordinate analysis (PCoA) to analyze beta diversity of microbial composition at the genus level. The beta diversities of the flora were significantly different among the groups, with that of the HGF group being closer to that of the CON group (Figure 2B and 2F). Further, we found that *Firmicutes* and *Bacteroidetes* dominated each group at the phylum level (Figure 2C and 2G). In the CKD group, there was a higher *Firmicutes/Bacteroidetes* (*F/B*) ratio, which was restored in the HGF-H group in the fourth week (Figure 2D and 2H).

Furthermore, we compared the differential bacteria between the CKD and HGF-H groups and found significant differences. In particular, the abundance of short-chain fatty acid (SCFA)-producing bacteria, such as *Prevotella* and *Bacteroides*, was significantly greater in the HGF-treated group after 4 weeks (Figure 2I), and that of *Bacteroides* and *Coprococcus* was greater in the HGF-H group in the eighth week (Figure 2J). In contrast, some conditional pathogenic bacteria, such as *Clostridia* and *Ruminococcus*, were enriched in the CKD group (Figure 2I and J). These results indicate that the intestinal microbial imbalance in CKD can be improved by HGF treatment, in a way that regulates the abundance of pathogenic and beneficial bacteria.

Oral HGF Improved Colonic Microenvironment of the CKD Rats

Further, we evaluated the effects of HGF on the colonic environment of rats with CKD. Although there was no obvious difference between the CON and CKD groups, oral HGF significantly increased average fecal weight (Figure 3A and B). Moreover, the HGF-treated groups exhibited a significantly less residual feces in the colon (Figure 3C and D). Compared with the CON group, CKD group showed changes in the structure of the colonic recess, surface irregularity and inflammatory cell infiltration (Figure 3E). Disruption of tight junctions in the colonic epithelium was further determined by immunofluorescence and RT-PCR. Although HGF did not significantly affect the mRNA expression of ZO-1 and occludin (Figure 3F), it significantly increased the mean fluorescence density of ZO-1+ (Figure 3G) and occludin+ (Figure 3H). This efficacy was dose dependent (Figure 3I). Similarly, TA treatment also significantly increased average fecal weight, tended to restore colon length, and reduced colon injury (Figure S2G–S2J). The results showed that HGF improved the colonic microenvironment by increasing colonic motility and repairing the colonic barrier.

HGF Intervention Reduced Systemic Inflammation in CKD Rats

The gut microbiota and colonic microenvironment play important roles in defense against external pathogenic factors. We then evaluated the effects of HGF on the systemic inflammatory responses in CKD rats. The CKD group showed significantly higher concentrations of TNF-α, IL-6 and IL-1β in the serum than normal rats. Although HGF-L did not significantly affect the levels of pro-inflammatory cytokines (Figure 4A–C), it significantly induced the secretion of IL-10 in the serum (Figure 4D). In contrast, HGF-H decreased the levels of inflammatory cytokines and increased IL-10 levels (Figure 4A–D).

HGF can also alleviate renal inflammation by inhibiting the NF-κB signaling pathway. HGF decreased the mRNA (Figure 5A–C) and protein (Figure 5D–F) expression of inflammation-related cytokines such as TNF-α, IL-6, and TGF-β1. NF-κB is a canonical signaling pathway involved in the activation of inflammation. NF-κB, p-NF-κB, and p-IκBα levels were increased in the CKD group, while the expression of IκBα was downregulated in the kidneys of CKD rats (Figure 5E). In contrast, HGF treatment reversed these changes in a concentration-dependent manner (Figure 5G and H). These data indicate that HGF can suppress CKD-induced systemic inflammation.

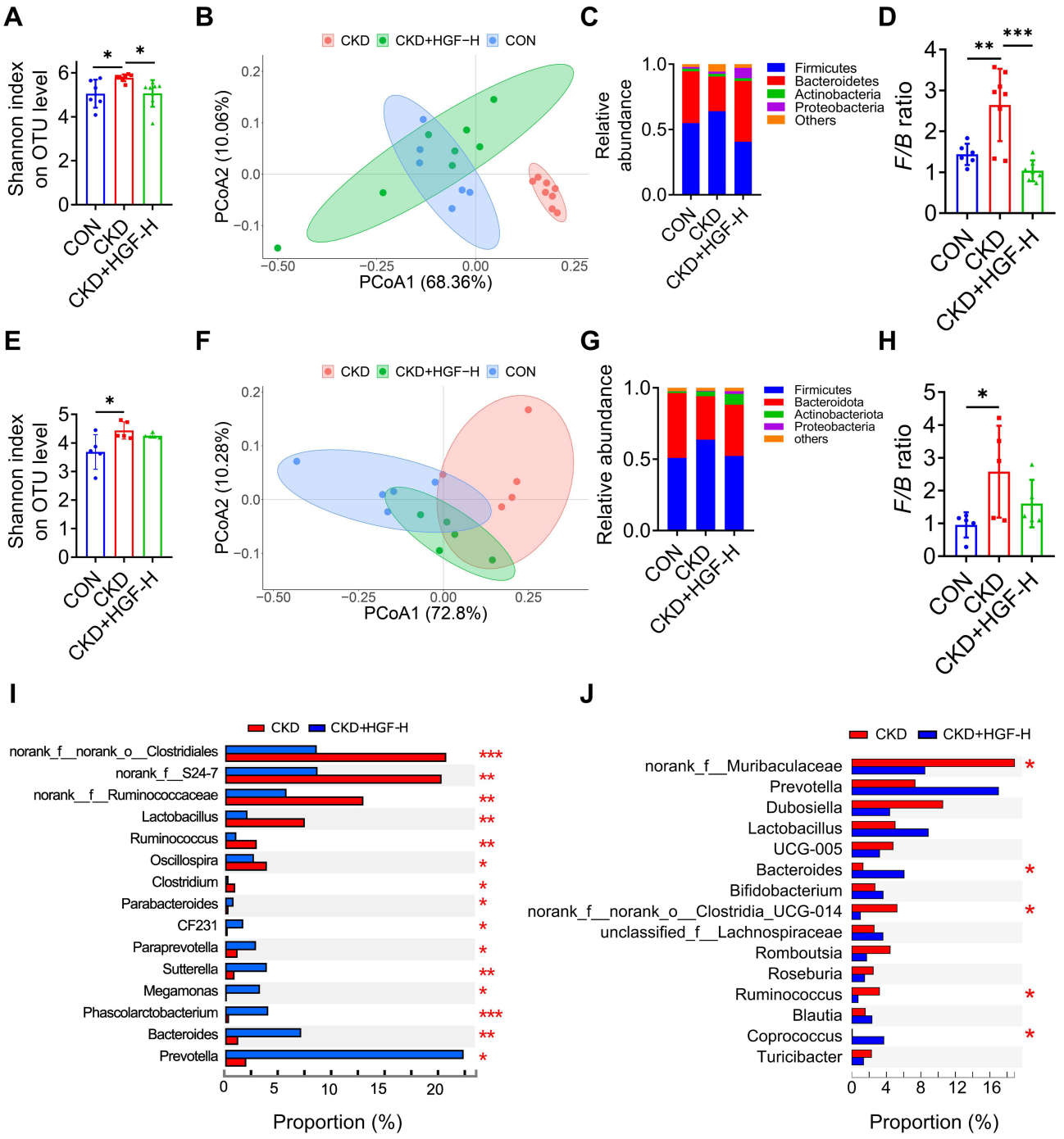

Figure 2 HGF improves the gut microbial dysbiosis in adenine-induced CKD. (**A**–**D**) In the 4th week, alpha diversity (**A**), beta diversity (**B**), relative abundance at the phylum level (**C**) and *Firmicutes*/*Bacteroidetes* (*F*/*B*) ratio (**D**) of the gut microbiota were analyzed. (**E**–**H**) In the 8th week, alpha diversity (**E**), beta diversity (**F**), relative abundance at the phylum level (**G**) and *F*/*B* ratio (**H**) of the gut microbiota were analyzed. (**I** and **J**) Relative abundance of differential bacteria between CKD and CKD + HGF-H group in the 4th (**I**) and 8th (**J**) weeks are shown with Wilcoxon rank-sum test bar plot. Red asterisk (*, **, ***) in (**I** and **J**) indicate $P < 0.05$, 0.01 or 0.001, respectively. n = 6–8 rats per group (4th week), and n = 5 rats per group (8th week). Data represent mean ± SD, *$P < 0.05$, **$P < 0.01$, and ***$P < 0.001$.

HGF Decreased the Risk of Uremia in Adenine-Induced CKD Rats

Recent studies have found that the altered structure and function of the gut flora in CKD may induce an increase in the levels of gut-derived toxins. In this study, the concentrations of well-studied toxins, such as indoxyl sulfate, *p*-cresol sulfate, advanced oxidation protein products and bacterial endotoxins, increased significantly compared with the CON group (Figure 6A–D). In contrast, high-dose HGF intervention decreased the levels of all selected uremic toxins in CKD

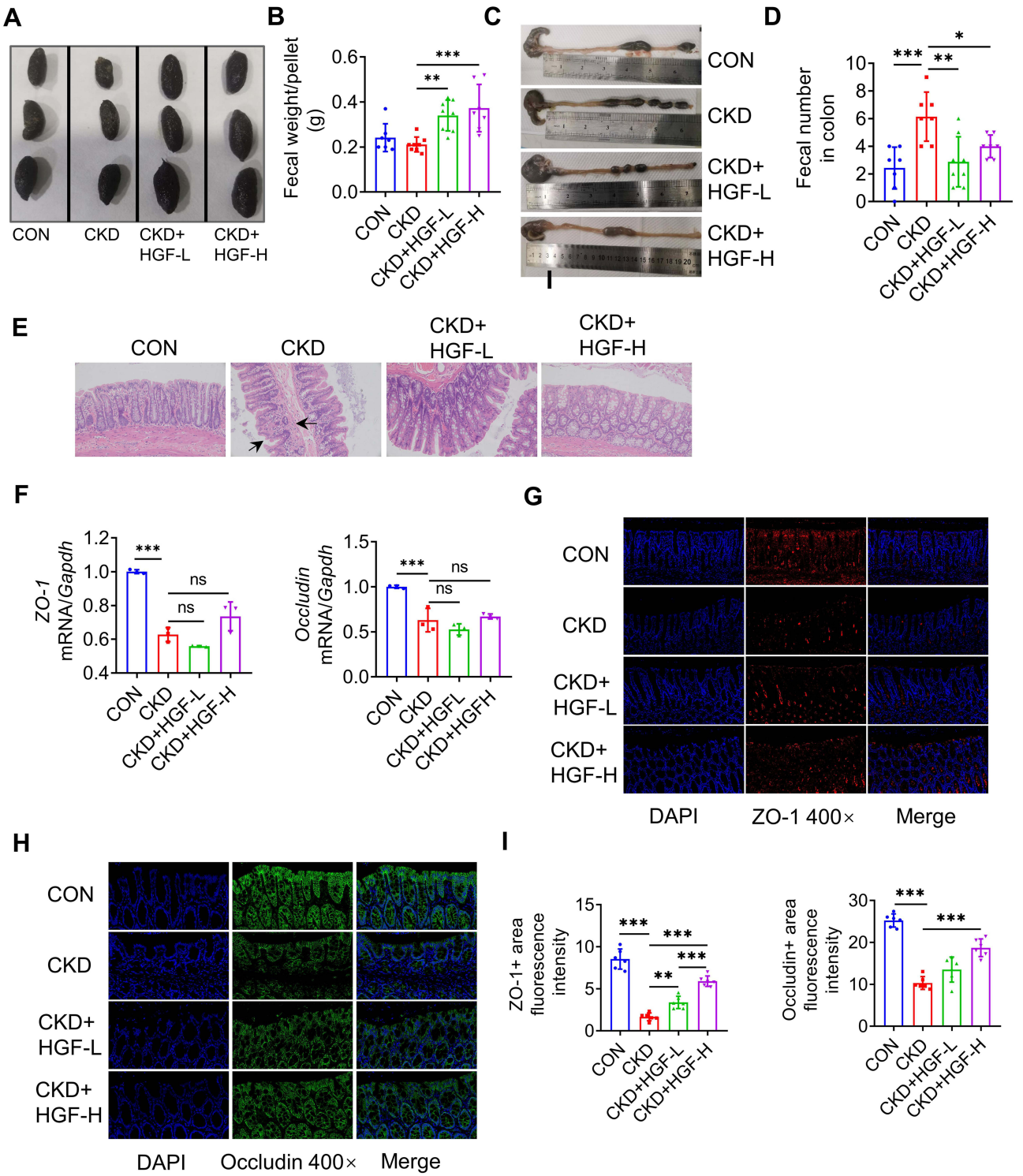

Figure 3 Effects of HGF on the colonic microenvironment in the CKD rats. (**A** and **B**) Fecal shape (**A**), and weight per pellet (**B**) that was calculated as (total wet weight) / (total numbers), n = 7–8 rats per group. (**C** and **D**) Number of residual stools in the colon, n = 7–8 rats per group. (**E**) Representative images of the colonic tissues using H&E stains (200×). The black arrows indicate injuries. (**F**) mRNA expression of ZO-1 and Occludin in colon tissues, n = 3 from three independent experiments. (**G** and **H**) Representative pictures of expression of ZO-1 and Occludin in colon from immunofluorescence staining (400×). (**I**) The mean fluorescence intensity of ZO-1 and occludin was quantified by ImageJ software, n = 6 rats per group. Data represent mean ± SD, **P* < 0.05, ***P* < 0.01, and ****P* < 0.001.

https://doi.org/10.2147/DDDT.S421446 DovePress

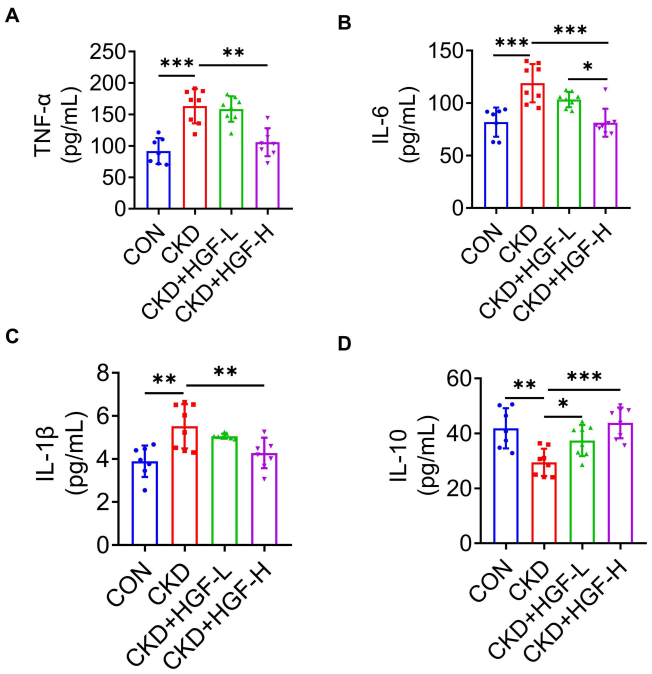

Figure 4 HGF suppresses blood's inflammation of the CKD rats. Concentration of TNF-α (**A**), IL-6 (**B**), IL-1β (**C**) and IL-10 (**D**) in rat serum were determined by ELISA, n = 7–8 rats per group. Data represent mean ± SD, **P* < 0.05, ***P* < 0.01, and ****P* < 0.001.

rats, whereas HGF-L only reduced the level of endotoxin. These results suggest that HGF can reduce the risk of uremia by decreasing the retention of toxic metabolites in blood.

HGF Alleviated Systemic Inflammation and Uremia Associated with Regulating the Gut Flora

As shown in Figure 7A, RDA analysis indicated that pro-inflammatory cytokines and uremic toxins were positively correlated, but they were all negatively correlated with the level of IL-10. Further, we generated an LDA bar graph and Spearman correlation heat map to determine the correlations between the differential microbiota (at the genus level) and inflammatory factors. *Prevotella, Ruminococcus*, and *Phascolarctobacterium* were enriched in the CON group (Figure 7B). The abundance of *Prevotella* was positively correlated with the expression of IL-10 and negatively correlated with all pro-inflammatory cytokines and uremic toxins (Figure 7C). In the CKD group, bacteria from families of *Muribaculaceae, Dubosiella, Romboutsia* and *Turicibacter* were positively correlated with all inflammatory and uremic toxins. The genera *Bacteroides, Coprococcus* and *Collinsella* were enriched in the HGF-H group and were nearly independent of inflammatory factors (Figure 7B and C). These results suggest that the increased abundance of conditional pathogenic bacteria is related to a worse blood environment, whereas a decrease in their percentage by HGF shows less CKD-associated systemic inflammation and uremia.

Discussion

Due to decreased renal function, CKD patients inevitably experience "toxins" accumulation in the body, which is an important risk factor for renal injury and its complications.[15,19,20] The "toxins" here are not limited to typical uremic toxins, but also include inflammatory cytokines. Disproportionately high levels of toxins in the blood were the main features of CKD-related systemic inflammation and uremia, which relates to microbial dysbiosis and barrier dysfunction.[5] Therefore, it can be beneficial for CKD treatment to regulate the gut microbiota and improve intestinal microenvironment.

In this study, adenine gavage resulted in significant weight loss and abnormal levels of biochemical indicators related to renal function (eg, BUN and SCR). Histopathological analysis revealed visible renal hypertrophy, extracellular matrix

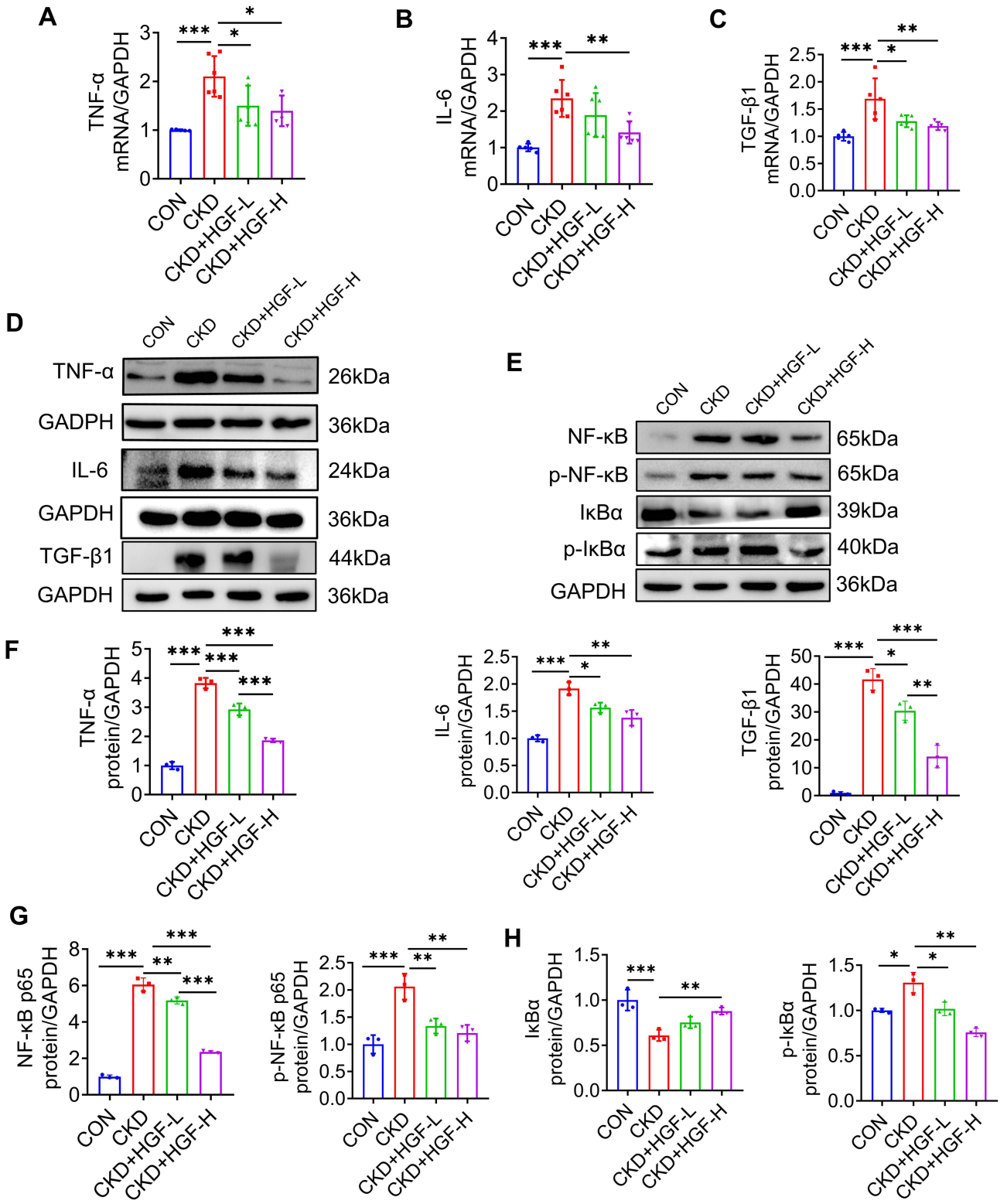

Figure 5 HGF alleviates renal inflammation by inhibiting NF-κB signaling pathway. (**A**–**C**) The mRNA expression of TNF-α (**A**), IL-6 (**B**) and TGF-β1 (**C**) in renal tissue were detected by RT-PCR. (**D** and **E**) The protein expression of TNF-α, IL-6, TGF-β1, NF-κB, p-NF-κB, IκBα, and p-IκBα in renal tissues were detected by Western blot. (**F**–**H**) Optical density of TNF-α, IL-6 and TGF-β1 (**F**), NF-κB and p-NF-κB (**G**), IκBα and p-IκBα (**H**) was quantified by ImageJ software, n = 3 rats per group. The visualization of the bands was performed by using Rapid Auto-exposure mode of the Image Lab™ Touch Software that supported by ChemiDoc™ System from the Bio-Rad. The exposure time for GAPDH was 3 to 10 second, while that for the tested proteins were a few seconds to several minutes. All data represent mean ± SD, **P* < 0.05, ***P* < 0.01, and ****P* < 0.001.

https://doi.org/10.2147/DDDT.S421446 DovePress

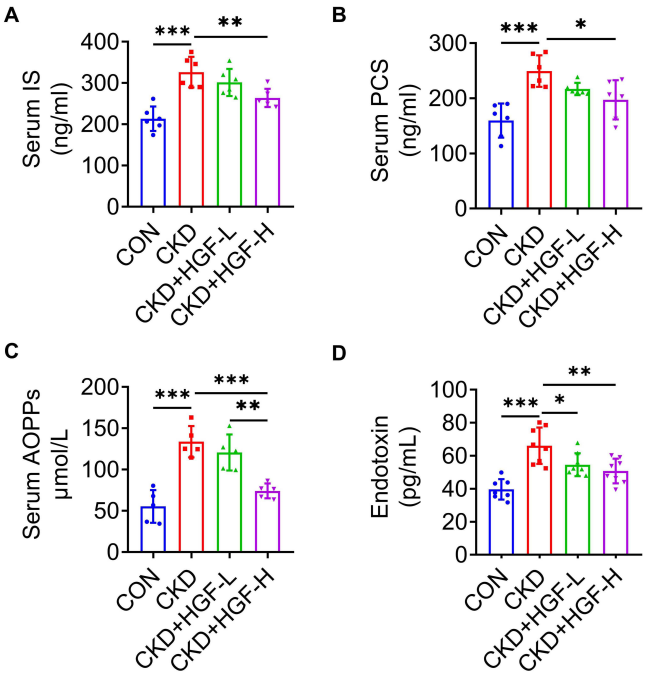

Figure 6 HGF reduces the level of uremic toxins in CKD. The concentration of indoxyl sulfate (IS) (**A**), *p*-cresol sulfate (PCS) (**B**), advanced oxidation products (AOPPs) (**C**), and endotoxin (**D**) were detected by ELISA, n = 5–6 rats per group. Data represent mean ± SD, **P* < 0.05, ***P* < 0.01, and ****P* < 0.001.

deposition and fibrosis in CKD rats. These lesions were consistent with the pathological manifestations reported in other studies.[18,21,22] However, HGF and its main ingredients both improved the indicators of renal structure and function after 8 weeks, which became the pharmacological basis of HGF in the treatment of CKD.

The mechanisms underlying HGF's renoprotection were further investigated. Different from the previous study, we emphasized the direct inhibition or reversal of renal fibrosis by suppressing the Wnt/β-catenin signaling pathway.[14] In this study, we focus on the effects of HGF on the gut–kidney interactions. Compared with the control group, the composition and structure of the gut flora were significantly altered in CKD rats. Among these alterations, the alpha diversity increased in the CKD group, which might be related to an increase in the abundance of some pathogenic bacteria. In fact, in patients with end-stage renal disease, there is an increased abundance of uremic toxin-producing microbes, such as *Clostridiaceae*.[23] As shown in Figure 2, *Clostridia_UCG-014* and *Clostridium* were enriched in CKD rats. They are considered to contain urease and form *p*-cresol through tryptophan metabolism.[23] Tryptophan metabolism is the main path through which the gut flora produces indole, a precursor of IS and PCS. IS and PCS are gut-derived toxins that contribute to the development of CKD and vascular disease via an induction of oxidative stress.[15,24] Beta diversity and *F/B* ratio also indicate that microbial community compositions between the CON and CKD groups are significantly different. Conversely, after HGF-H treatment, both alpha and beta diversities in CKD rats were corrected. Moreover, HGF-H increased the abundance of *Prevotella, Bacteroides* and *Coprococcus* that involve in producing short chain fatty acids. SCFAs, which are mainly fermented by bacteria in the colon, are reported to exhibit anti-inflammatory and anti-oxidation.[25] They have also been found to be beneficial for renal diseases, and direct drinking water containing SCFAs can improve adenine-induced CKD.[26] Together, these results suggest that HGF can correct the intestinal microbiota imbalance in CKD by regulating the abundance of pathogenic and beneficial bacteria.

In CKD mice induced by adenine, gastrointestinal transit time is prolonged,[27] which relates to immune activation and inflammation in the intestine.[28] This may be caused by an increase in pathogenic bacteria and toxins in the colonic lumen; however, reducing their retention times may be beneficial. For example, lubiprostone, a drug used to treat chronic constipation, can alleviate renal inflammation and fibrosis in CKD.[29] Similarly, rhubarb is a traditional Chinese herb that is used to treat constipation, it has been developed for the treatment of CKD-related intestinal flora imbalance in recent years.[12] Of note, rhubarb is the major ingredient in HGF, and this is why we choose the quantity of rhubarb

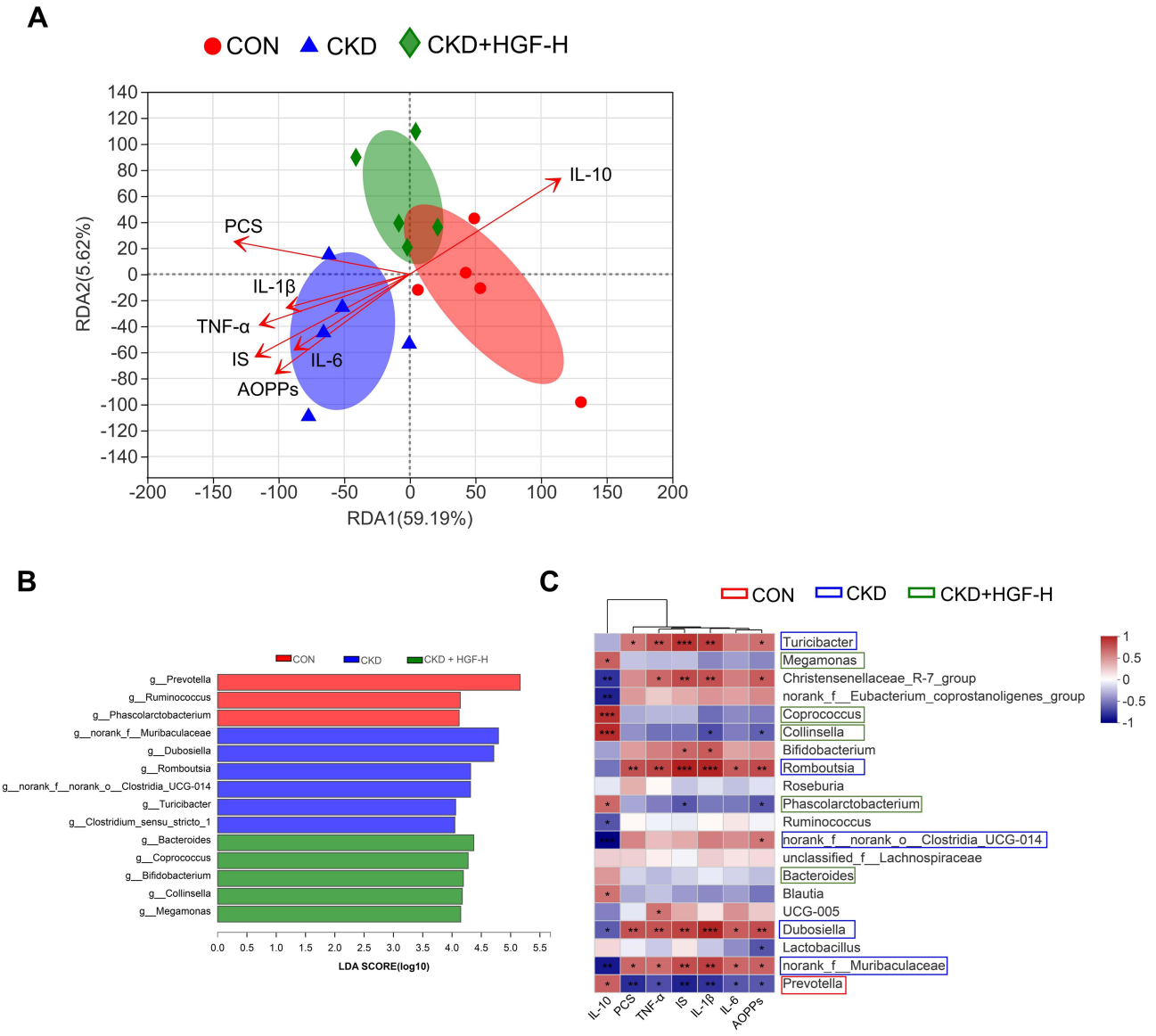

Figure 7 HGF suppresses systemic inflammation and uremia by regulating the intestinal flora. (**A**) RDA plots show relationship between the selected cytokines. (**B**) The bacteria enriched in groups was determined using linear discriminant analysis. (**C**) Spearman correlation heatmap presents correlations between the gut flora, inflammatory cytokines and uremic toxins. *P*-values of the correlation were shown: **P* < 0.05, ***P* < 0.01, and ****P* < 0.001.

anthraquinones as quality control of this study. Toxins increase in lumen and fail to be excreted, increasing the time it takes for toxins to interact with intestinal epithelial cells. Increased intestinal permeability allows bacterial endotoxins to enter the blood, which are captured by immune cells, such as macrophages, and TNF-α and IL-6 are secreted.[10] This process should be protective in the early stages of pathogen invasion; however, it can cause systemic inflammation when unresolved. Thus, renal injury and intestinal dysfunction begin and amplify each other. HGF treatment increased colonic motility and promoted fecal excretion from the lumen. HGF also increases the expression of tight junctions, thus reducing the entry of bacterial endotoxins into the blood. The results indicate that HGF can improve colonic micro-environment of CKD.

Intestinal microbial dysbiosis and barrier dysfunction highly relates to systemic inflammation and uremia in CKD.[30] CKD-related inflammation is characterized by high levels of inflammatory cytokines in the renal tissue and circulatory system. Firstly, we found that HGF significantly reduced the levels of inflammatory cytokines in serum of CKD rats. Secondly, renal damage recruits innate immune cells to the injury site, which can amplify the inflammatory response by

activating the NF-κB pathway.[31] When inactivated, NF-κB is bound by IκBα in the cytoplasm. Once triggered by stimulation (eg, TNF-α and IL-6), phosphorylated IκBα is rapidly degraded by the ubiquitin proteasome pathway, which leads to the translocation of NF-κB into the nucleus, allowing it to regulate downstream gene expression.[32] In the CKD group, significantly increased expression of TNF-α, IL-6 and TGF-β1 was observed in the renal tissues, and the NF-κB pathway was activated. However, HGF inhibited the phosphorylation of NF-κB and IκBα, but conversely promoted the expression of IκBα that restrain the translocation of NF-κB into the nucleus. These results suggest that HGF can reduce renal inflammation and fibrosis via suppressing NF-κB pathway.

Increased level of IS was reported to inhibit the expression of tight junction in colonic epithelial cells. In contrast, AST-120 (an oral adsorbent for IS) administration attenuated IS-induced intestinal barrier injury in CKD mice.[9] AOPPs are novel protein-bound uremic toxins that are significantly produced in the process of various chronic kidney diseases.[33] AOPPs is a biomarker of inflammation and can induce renal fibrosis through epidermal mesenchymal transition of renal tubular cell.[34] AOPPs also change the activity and expression of drug metabolism enzymes,[35] which interferes with the drug treatment of CKD. Our results suggest that HGF (especially high dose) reduces the levels of uremic toxins, which are believed to alleviate the notorious effects of these toxins.

Finally, the relationship between inflammation, uremia and the changed gut microbiota was further determined by correlation analysis. In the CKD rats, there are more harmful microbes that positively correlated with inflammatory and uremic toxins. However, in the HGF-H group, there are more beneficial bacteria, such as *Prevotella* that was negatively correlated with inflammatory cytokines and uremic toxins but positively correlated with anti-inflammatory cytokine. These results indicate that HGF may regulate the gut microbiota to alleviate systemic inflammation and uremia.

Conclusion

In summary, a deteriorated intestinal environment may induce systemic inflammation and increase the risk of uremia, which has become more significant in the progression of chronic kidney disease. This study demonstrated that HGF can improve CKD outcomes by alleviating systemic inflammation and uremia. These effects can be explained by the regulation of the gut flora and colonic microenvironment.

Data Sharing Statement

The original figures and tables used to support the findings of this study have been included in this article. Raw sequencing data can be identified in the NCBI Sequence Read Archive (accession number PRJNA847394).

Acknowledgments

This research was funded by Technology Project of Guangdong Province (2015B020211006), Technology Project (201604020137) of Guangzhou City in China, Province Natural Science Fund of Guangdong (2020A1515011327), Traditional Chinese Medicine Bureau of Guangdong Province (20221273), and Shenzhen Foundation of Science and Technology (JCYJ20190814112205770) and (JCYJ20230807151308018O).

Author Contributions

All authors made a significant contribution to the work reported, whether that is in the conception, study design, execution, acquisition of data, analysis and interpretation, or in all these areas; took part in drafting, revising or critically reviewing the article; gave final approval of the version to be published; have agreed on the journal to which the article has been submitted; and agree to be accountable for all aspects of the work.

Disclosure

The authors declare no conflict of interest.

References

1. Ruiz-Ortega M, Rayego-Mateos S, Lamas S, Ortiz A, Rodrigues-Diez RR. Targeting the progression of chronic kidney disease. *Nat Rev Nephrol*. 2020;16(5):269–288. doi:10.1038/s41581-019-0248-y
2. Joachim J, Jürgen F, Danilo F, Michael B, Nikolaus M. Cardiovascular disease in chronic kidney disease: pathophysiological insights and therapeutic options. *Circulation*. 2021;143:11.
3. Yeung CK, Shen DD, Thummel KE, Himmelfarb J. Effects of chronic kidney disease and uremia on hepatic drug metabolism and transport. *Kidney Int*. 2014;85(3):522–528. doi:10.1038/ki.2013.399
4. Impellizzeri D, Esposito E, Attley J, Cuzzocrea S. Targeting inflammation: new therapeutic approaches in chronic kidney disease (CKD). *Pharmacol Res*. 2014;81:91–102. doi:10.1016/j.phrs.2014.02.007
5. Andersen K, Kesper MS, Marschner JA, et al. Intestinal dysbiosis, barrier dysfunction, and bacterial translocation account for CKD-related systemic inflammation. *J Am Soc Nephrol*. 2017;28(1):76–83. doi:10.1681/ASN.2015111285
6. Onal EM, Afsar B, Covic A, Vaziri ND, Kanbay M. Gut microbiota and inflammation in chronic kidney disease and their roles in the development of cardiovascular disease. *Hypertens Res*. 2019;42(2):123–140. doi:10.1038/s41440-018-0144-z
7. Mafra D, Lobo JC, Barros AF, et al. Role of altered intestinal microbiota in systemic inflammation and cardiovascular disease in chronic kidney disease. *Future Microbiol*. 2014;9(3):399–410. doi:10.2217/fmb.13.165
8. Hobby GP, Karaduta O, Dusio GF, et al. Chronic kidney disease and the gut microbiome. *Am J Physiol Renal Physiol*. 2019;316(6):F1211–f7. doi:10.1152/ajprenal.00298.2018
9. Huang Y, Zhou J, Wang S, et al. Indoxyl sulfate induces intestinal barrier injury through IRF1-DRP1 axis-mediated mitophagy impairment. *Theranostics*. 2020;10(16):7384–7400. doi:10.7150/thno.45455
10. Andrade-Oliveira V, Foresto-Neto O, Watanabe IKM, Zatz R, Câmara NOS. Inflammation in renal diseases: new and old players. *Front Pharmacol*. 2019;10:1192. doi:10.3389/fphar.2019.01192
11. Yue SJ, Wang WX, Yu JG, et al. Gut microbiota modulation with traditional Chinese medicine: a system biology-driven approach. *Pharmacol Res*. 2019;148:104453. doi:10.1016/j.phrs.2019.104453
12. Wang R, Hu B, Ye C, et al. Stewed rhubarb decoction ameliorates adenine-induced chronic renal failure in mice by regulating gut microbiota dysbiosis. *Front Pharmacol*. 2022;13:842720. doi:10.3389/fphar.2022.842720
13. Deng Q, Bu C, Mo L, et al. Huang gan formula eliminates the oxidative stress effects of advanced oxidation protein products on the divergent regulation of the expression of AGEs receptors via the JAK2/STAT3 pathway. *Evid Based Complement Alternat Med*. 2017;2017:4520916. doi:10.1155/2017/4520916
14. Mo L, Xiao X, Song S, et al. Protective effect of Huang Gan formula in 5/6 nephrectomized rats by depressing the Wnt/β-catenin signaling pathway. *Drug Des Devel Ther*. 2015;9:2867–2881. doi:10.2147/DDDT.S81157
15. Cheng TH, Ma MC, Liao MT, et al. Indoxyl sulfate, a tubular toxin, contributes to the development of chronic kidney disease. *Toxins*. 2020;12(11):684. doi:10.3390/toxins12110684
16. Xun T, Lin Z, Zhan X, et al. Advanced oxidation protein products upregulate efflux transporter expression and activity through activation of the Nrf-2-mediated signaling pathway in vitro and in vivo. *Eur J Pharm Sci*. 2020;149:105342. doi:10.1016/j.ejps.2020.105342
17. Zhu H, Cao C, Wu Z, et al. The probiotic L. casei Zhang slows the progression of acute and chronic kidney disease. *Cell Metab*. 2021;33(10):1926–42.e8. doi:10.1016/j.cmet.2021.06.014
18. Zhou F, Zou X, Zhang J, et al. Jian-Pi-Yi-shen formula ameliorates oxidative stress, inflammation, and apoptosis by activating the Nrf2 signaling in 5/6 nephrectomized rats. *Front Pharmacol*. 2021;12:630210. doi:10.3389/fphar.2021.630210
19. Gouroju S, Rao P, Bitla AR, et al. Role of gut-derived uremic toxins on oxidative stress and inflammation in patients with chronic kidney disease. *Indian J Nephrol*. 2017;27(5):359–364. doi:10.4103/ijn.IJN_71_17
20. Zhang W, Miikeda A, Zuckerman J, et al. Inhibition of microbiota-dependent TMAO production attenuates chronic kidney disease in mice. *Sci Rep*. 2021;11(1):518. doi:10.1038/s41598-020-80063-0
21. Cai H, Su S, Li Y, et al. Danshen can interact with intestinal bacteria from normal and chronic renal failure rats. *Biomed Pharmacother*. 2019;109:1758–1771. doi:10.1016/j.biopha.2018.11.047
22. Zhang ZM, Yang L, Wan Y, et al. Integrated gut microbiota and fecal metabolomics reveal the renoprotective effect of rehmanniae radix preparata and corni fructus on adenine-induced CKD rats. *J Chromatogr B Analyt Technol Biomed Life Sci*. 2021;1174:122728. doi:10.1016/j.jchromb.2021.122728
23. Wong J, Piceno YM, DeSantis TZ, et al. Expansion of urease- and uricase-containing, indole- and p-cresol-forming and contraction of short-chain fatty acid-producing intestinal microbiota in ESRD. *Am J Nephrol*. 2014;39(3):230–237. doi:10.1159/000360010
24. Yu M, Kim YJ, Kang DH. Indoxyl sulfate-induced endothelial dysfunction in patients with chronic kidney disease via an induction of oxidative stress. *Clin J Am Soc Nephrol*. 2011;6(1):30–39. doi:10.2215/CJN.05340610
25. Koh A, De Vadder F, Kovatcheva-Datchary P, Bäckhed F. From dietary fiber to host physiology: short-chain fatty acids as key bacterial metabolites. *Cell*. 2016;165(6):1332–1345. doi:10.1016/j.cell.2016.05.041
26. Mikami D, Kobayashi M, Uwada J, et al. Short-chain fatty acid mitigates adenine-induced chronic kidney disease via FFA2 and FFA3 pathways. *Biochim Biophys Acta Mol Cell Biol Lipids*. 2020;1865(6):158666. doi:10.1016/j.bbalip.2020.158666
27. Hoibian E, Florens N, Koppe L, Vidal H, Soulage CO. Distal colon motor dysfunction in mice with chronic kidney disease: putative role of uremic toxins. *Toxins*. 2018;10(5):204. doi:10.3390/toxins10050204
28. Khalif IL, Quigley EM, Konovitch EA, Maximova ID. Alterations in the colonic flora and intestinal permeability and evidence of immune activation in chronic constipation. *Dig Liver Dis*. 2005;37(11):838–849. doi:10.1016/j.dld.2005.06.008
29. Mishima E, Fukuda S, Shima H, et al. Alteration of the intestinal environment by lubiprostone is associated with amelioration of adenine-induced CKD. *J Am Soc Nephrol*. 2015;26(8):1787–1794. doi:10.1681/ASN.2014060530
30. Rukavina Mikusic NL, Kouyoumdzian NM, Choi MR. Gut microbiota and chronic kidney disease: evidences and mechanisms that mediate a new communication in the gastrointestinal-renal axis. *Pflugers Arch*. 2020;472(3):303–320. doi:10.1007/s00424-020-02352-x
31. Tang PC, Zhang YY, Chan MK, et al. The emerging role of innate immunity in chronic kidney diseases. *Int J Mol Sci*. 2020;21(11):4018. doi:10.3390/ijms21114018

32. Thompson JE, Phillips RJ, Erdjument-Bromage H, Tempst P, Ghosh S. I kappa B-beta regulates the persistent response in a biphasic activation of NF-kappa B. *Cell*. 1995;80(4):573–582. doi:10.1016/0092-8674(95)90511-1
33. Li HY, Hou FF, Zhang X, et al. Advanced oxidation protein products accelerate renal fibrosis in a remnant kidney model. *J Am Soc Nephrol*. 2007;18(2):528–538. doi:10.1681/ASN.2006070781
34. Feng H, Hu H, Zheng P, et al. AGE receptor 1 silencing enhances advanced oxidative protein product-induced epithelial-to-mesenchymal transition of human kidney proximal tubular epithelial cells via RAGE activation. *Biochem Biophys Res Commun*. 2020;529(4):1201–1208. doi:10.1016/j.bbrc.2020.06.144
35. Xun T, Lin Z, Zhang M, et al. Advanced oxidation protein products upregulate ABCB1 expression and activity via HDAC2-Foxo3α-mediated signaling in vitro and in vivo. *Toxicol Appl Pharmacol*. 2022;449:116140. doi:10.1016/j.taap.2022.116140